Computational and Theoretical Chemistry 1104 (2017) 32–36

Contents lists available at ScienceDirect

Computational and Theoretical Chemistry

journal homepage: www.elsevier.com/locate/comptc

Nonlinear dynamics of picosecond pulse trains in naphthalocyanines and phthalocyanines

Quan Miao [a,*], Erping Sun [a], Min Liang [a,b], Qixin Liu [a,b], Yan Xu [a,b]

[a] College of Electronics, Communication and Physics, Shandong University of Science and Technology, Qingdao, 266590 Shandong, People's Republic of China
[b] College of Electrical Engineering and Automation, Shandong University of Science and Technology, Qingdao, 266590 Shandong, People's Republic of China

ARTICLE INFO

Article history:
Received 5 January 2017
Received in revised form 2 February 2017
Accepted 3 February 2017
Available online 6 February 2017

Keywords:
Pulse trains
Optical limiting
Naphthalocyanine
Phthalocyanine
Reverse saturable absorption

ABSTRACT

We study the optical dynamics of picosecond pulse trains in naphthalocyanines and phthalocyanines. The pulse train is assumed to contain 35 ps subpulses with each subpulse width of 100 ps and with spacing between subpulses of 12 ns. In this work, we used numerical theoretical method by solving two-dimensional paraxial filed equation coupled with rate equations. Molecular parameters are extracted from experiments and our results show good consistency with the experimental work. The dynamical processes in naphthalocyanines and phthalocyanines are simulated with a five-level model, where the main optical mechanism is the sequential (singlet-singlet) × (triplet-triplet) two-photon absorption. The results of this work emphasize that both naphthalocyanines and phthalocyanines are good optical limiting materials, and naphthalocyanine with lighter central metal Ga shows better optical behaviour with picosecond pulse trains.

1. Introduction

Nowadays, laser technology has got extremely rapid development and it has been widely used in various fields such as medicine, communication, military and many other influential fields [1]. The widespread applications of laser gradually give rise to one important issue, which is the protection of optical devices and human eyes from the strong intensity laser. One of the most efficient method is to adopt optical limiting (OL) materials for protection [2,3]. Until now, reverse saturable absorption (RSA) is the most frequently used one among various mechanisms to achieve OL function [4–6]. The absorption cross section of excited state is larger than that of ground state, which is the main characteristic of RSA materials [7–9].

The OL dynamics are mainly determined by the duration of interaction between laser pulses and materials. For ultrashort pulses such as femtosecond pulses, the primary OL absorption process is the one-step coherent two-photon absorption (TPA). But for long laser pulses such as nanosecond pulses or laser pulse trains, two-step sequential TPA dominates the OL absorption where RSA is the main OL mechanism. In this case, the light-matter interaction requires a finite response time [10–13]. So for those materials with singlet and triplet states, the principal absorption channel is the sequential (singlet-singlet) × (triplet-triplet) TPA [4]. The duration of laser pulses could be comparable with the effective population transfer time which is known as the transfer time from ground to triplet state.

In the course of finding and synthesizing better RSA materials, naphthalocyanines (Npcs) and phthalocyanines (Pcs) attract thousands of researchers. The main advantage lies in their special structure with highly conjugated delocalized π-electron [14–22]. One recent experiment reported their OL and photophysical study of Npcs and Pcs with different central metal-coordination bond [23]. Our previous work has theoretically studied Npcs and Pcs based on the experiment with single nanosecond laser pulses [24]. In this work we focus on the nonlinear dynamics of picosecond pulse trains in Npcs and Pcs by numerically solving the paraxial field equation together with the rate equations [25].

2. Method

The molecular structures of Npcs and Pcs are shown in Fig. 1(a). Considering the interaction between picosecond pulse trains and Npcs and Pcs, we simplified the system to be a five-level scheme as shown in Fig. 1(b). Since we considered long pulses, so there are two sequential TPA channels in this scheme: $(S_0 \rightarrow S_1) \times (S_1 \rightarrow S_n)$ and $(S_0 \rightarrow S_1) \times (T_1 \rightarrow T_2)$. Also we assumed the frequency of pulse trains to be in the vicinity of one-photon transitions in accordance with the experiment [23].

* Corresponding author.
E-mail address: qmiao2013@yahoo.com (Q. Miao).

http://dx.doi.org/10.1016/j.comptc.2017.02.004
2210-271X/

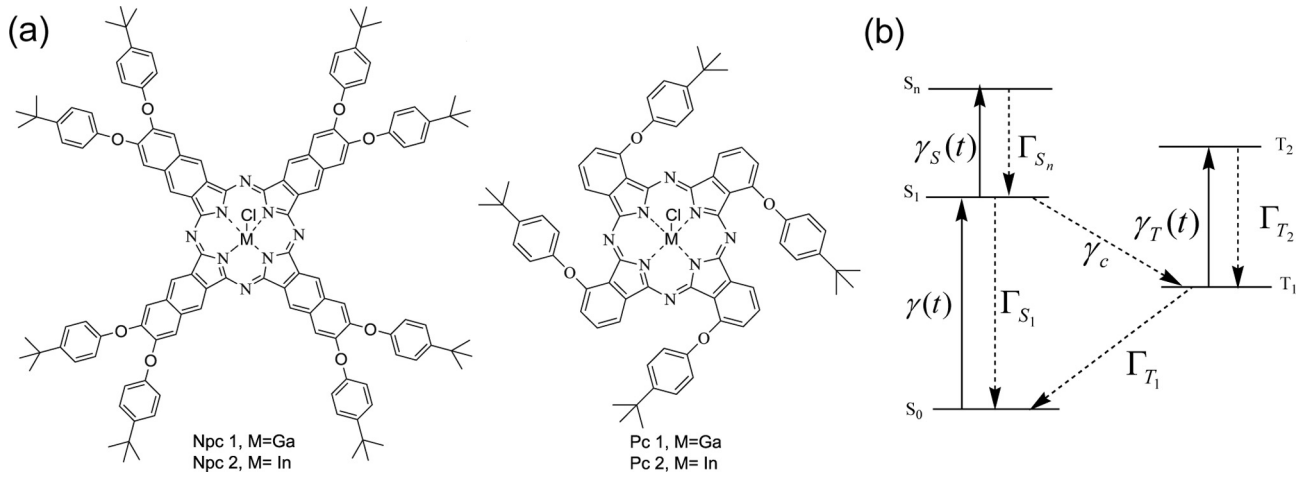

Fig. 1. (a) Structures of the naphthalocyanines and phthalocyanines in Ref. [23] and (b) the Jablonski diagram of a generalized five-level system.

The incident laser pulse train is supposed as

$$I(t) = \sum_{n=0} I_n(t), \quad n = 0, 1, \ldots, n_{tot} - 1, \tag{1}$$

where n is the subpulse number starting from 0, n_{tot} is the total subpulses number.

For each subpulse, the paraxial equation can be described in the following form [26]

$$\left(\frac{\partial}{\partial z} - \frac{1}{c}\frac{\partial}{\partial t}\right) I_n(t) = -N \sum_{j>i} \sigma_{ij}(\rho_i - \rho_j) I_n(t), \tag{2}$$

where N is molecular concentration, σ_{ij} is absorption cross-section via transition from state i to state j. Here c is the speed of light in vacuum, z is the propagation distance and ρ_k is the population of state k.

Under the interaction of laser pulses, the dynamical populations of the five states can be described by the rate equations [27],

$$\begin{aligned}
&\frac{\partial}{\partial t}\rho_{S_0} = -\gamma(t)(\rho_{S_0} - \rho_{S_1}) + \Gamma_{S_1}\rho_{S_1} + \Gamma_{T_1}\rho_{T_1},\\
&\left(\frac{\partial}{\partial t} + \Gamma_{S_1} + \gamma_c\right)\rho_{S_1} = \Gamma_{S_n}\rho_{S_n} - \gamma_S(t)(\rho_{S_1} - \rho_{S_n}) + \gamma(t)(\rho_{S_0} - \rho_{S_1}),\\
&\left(\frac{\partial}{\partial t} + \Gamma_{S_n}\right)\rho_{S_n} = \gamma_S(t)(\rho_{S_1} - \rho_{S_n}),\\
&\left(\frac{\partial}{\partial t} + \Gamma_{T_2}\right)\rho_{T_2} = \gamma_T(t)(\rho_{T_1} - \rho_{T_2}), \quad \sum_k \rho_k = 1,
\end{aligned} \tag{3}$$

where γ_c is the rate of intersystem crossing (ISC) transition $S_1 \to T_1$. $\Gamma_{S_1}, \Gamma_{S_n}, \Gamma_{T_1}$ and Γ_{T_2} are the decay rates of the states S_1, S_n, T_1 and T_2, respectively. $\gamma(t), \gamma_S(t)$ and $\gamma_T(t)$ are the populated rates to higher states via one-photon transitions $S_0 \to S_1, S_1 \to S_n$ and $T_1 \to T_2$ respectively, which can be written as

$$\gamma_{ij}(t) = \frac{\sigma_{ij} I(t)}{\hbar\omega}, \tag{4}$$

where ω is the laser frequency. Here $\hbar = h/(2\pi)$, $h = 6.626 \times 10^{-34}$ is Planck constant.

In our work, we supposed the pulse train has 35 subpulses with each subpulse width of 100 ps and with spacing between subpulses of 12 ns. Also we assumed the temporal shape of the initial subpulse has rectangular form, which could characterize the shape of subpulses more accurately [26,28].

$$I_n(r) = I_0 \exp\left[-\left(\frac{n\Delta - t_0}{\tau_e}\right)^2 \ln 2\right] \exp\left[-\left(\frac{r}{r_0}\right)^2 \ln 2\right], \tag{5}$$

where $t_0 = [(n_{tot} - 1)\Delta + \tau]/2$, $\tau_e = 10\Delta/3$ is the half width at half-maximum (HWHM) of the envelope, $r_0 = 2$ mm is the beam width. The pulse trains used in experiments are usually picosecond pulses separated by nanosecond separation [9,29,30]. In experiment [23], the single pulse duration is 3.5 ns (HWHM). In our simulation, we assumed $\Delta = 12$ ns, $\tau = 100$ ps, and $n_{tot} = 35$, so the total duration of all laser subpulses is also 35×100 ps $= 3.5$ ns.

To better study the OL process, we also calculated the energy transmittance,

$$\mathcal{T}(L) = \frac{J(z_0 + L)}{J(z_0)}, \tag{6}$$

where $z_0 = 0$ is the entry position of the pulse train, L is the thickness of materials. $J(z_0)$ and $J(z_0 + L)$ are the total pulse energy at z_0 and at $z_0 + L$ respectively. And the total pulse energy is written as

$$J(z) = 2\pi \int_0^R \int_0^\infty I(t, r, z) r dr dt, \tag{7}$$

where $I(t, r, z)$ is the instantaneous intensity.

3. Results and discussion

In order to ensure high reliability of our numerical results, we performed the simulations using photophysical parameters from the experiment [23], which are listed in Table 1. All samples in the experiment [23] were placed in a 1.0 cm path length quartz cell with concentration of 3.01×10^{22} m^{-3}. According to the scaling relation $L_{\text{theo}} N_{\text{theo}} = L_{\text{exp}} N_{\text{exp}}$, we reduced the length to $L_{\text{theo}} = 1.0$ mm and increased the concentration to $N_{\text{theo}} = 3.01 \times 10^{23}$ m^{-3}, which can highly save the computational expense. And we assumed $\Gamma_{S_n}^{-1} = \Gamma_{T_2}^{-1} = 1$ ps, $\Gamma_{S_1} + \gamma_c \approx \gamma_c$ and $\sigma_{S_1 S_n} = 10^{-21}$ m^2 in simulations.

The energy transmittances of the pulse train are quite important to analyze the OL dynamics of Npcs and Pcs which are shown in Figs. 2 and 3. In our simulations, the maximum peak of the incident pulse trains is set to be $I_0 = 1 \times 10^{13}$ W/m^2 which can avoid $S_0 \to S_1$ saturation absorption. In Fig. 2 with $I_0 = 1 \times 10^{13}$ W/m^2, one can see that both Npcs and Pcs display remarkable OL behaviours. The primary reason is the molecular structure with highly conjugated delocalized π-electron which is enhanced by the central metals. Also one can notice that Npcs show much better OL performance than Pcs along with the distance increasing. This is because Npcs with bulky substituents have one order of magnitude faster ISC rate γ_c than that of Pcs. So the sequential (singlet-singlet) × (triplet-triplet) TPA in Npcs is stronger than that in Pcs. With the increase of propagation distance, Npcs reach their saturation values of energy transmittances at about $L = 1.0$ mm which is much shorter than that for Pcs at $L = 2.0$ mm. According to the